자원환경지질, 제35권, 제2호, 273-284, 2002
Econ. Environ. Geol., 35(2), 273-284, 2002

Gravity-Geologic Prediction of Bathymetry in the Drake Passage, Antarctica

Jeong Woo Kim[1]*, Seong-Jae Doh[2], Sang Heon Nam[3], Soonwook Youn[2], and Young Keun Jin[3]

[1]Dept. of Geoinformation Sciences and Research Inst. of Geoinformatics & Geophysics, Sejong University, Korea
[2]Dept. of Earth and Environmental Sciences, Korea University, Korea
[3]Polar Research Division, Korea Ocean Research & Development Institute, Korea

Gravity-Geologic Method를 이용한 남극 드레이크 해협의 해저지형 연구

김정우[1]* · 도성재[2] · 남상헌[3] · 윤순욱[2] · 진영근[3]

[1]세종대학교 지구정보과학과 지구정보연구소, [2]고려대학교 지구환경과학과, [3]한국해양연구원 극지연구본부

인공위성 레이더고도 측정값으로부터 유도된 중력이상으로부터 남극 드레이크해협의 해저지형을 계산하기 위해 Gravity-Geologic Method(GGM)를 적용하였다. 총 6548개의 음향측심자료 중 2/3는 control depth로, 나머지는 결과 검증을 위한 check point 자료로 이용하였다. 효과적인 계산을 위해 해수와 해저지형의 밀도차이는 check point를 이용, 9.0 gm/cm^{3}로 가정하였다. Control depth로부터 광역중력이상을 계산하였고, 이를 Sandwell & Smith(1997)의 중력이상으로부터 제거하여 해저지형의 기복에 의한 중력 효과를 계산하였으며, 이로부터 해저지형을 복원하였다. Selective Merging 기법을 개발하여 복원된 해저지형과 고주파 측심자료를 효과적으로 합성하였다. 복원된 해저지형은 한국해양연구원의 측심자료, GEODAS 및 전지구 모델 ETOPO5 결과와 각각 0.91, 0.92, 0.85의 상관계수를 갖으며, Selective Merging을 이용한 최종 결과는 GEODAS 및 Smith & Sandwell(1997)의 결과와 각각 0.948 및 0.954의 상관관계 및 449.8, 441.3 m의 RMS 오차를 갖는다. GGM을 이용하여 계산된 해저지형은 측심이 충분히 이루어지지 않은 지역의 경우 전지구모델(ETOPO5)이나 자료의 양이 불충분한 음향측심에 의한 결과보다 우수한 것으로 나타났다.

주요어 : Gravity-Geologic Method, 해저지형복원, 레이더고도 중력이상, 남극 드레이크해협

The Gravity-Geologic Method (GGM) was implemented for bathymetric determinations in the Drake Passage, Antarctica, using global marine Free-air Gravity Anomalies (FAGA) data sets by Sandwell and Smith (1997) and local echo sounding measurements. Of the 6548 bathymetric sounding measurements, two thirds of these points were used as control depths, while the remaining values were used as checkpoints. A density contrast of 9.0 gm/cm^3 was selected based on the checkpoints predictions with changes in the density contrast assumed between the seawater and ocean bottom topographic mass. Control depths from the echo soundings were used to determine regional gravity components that were removed from FAGA to estimate the gravity effects of the bathymetry. These gravity effects were converted to bathymetry by inversion. In particular, a selective merging technique was developed to effectively combine the echo sounding depths with the GGM bathymetry to enhance high frequency components along the shipborne sounding tracklines. For the rugged bathymetry of the research area, the GGM bathymetry shows correlation coefficients (CC) of 0.91, 0.92, and 0.85 with local shipborne sounding by KORDI, GEODAS, and a global ETOPO5 model, respectively. The enhanced GGM by selective merging shows imploved CCs of 0.948 and 0.954 with GEODAS and Smith & Sandwell (1997)'s predictions with RMS differences of 449.8 and 441.3 meters. The global marine FAGA data sets and other bathymetric models ensure that the GGM can be used in conjunction with shipborne bathymetry from echo sounding to extend the coverage into the unmapped regions, which should generate better results than simply gridding the sparse data or relying upon lower resolution global data sets such as ETOPO5.

Key words : Gravity-Geologic Method, bathymetry prediction, altimetry-implied gravity anomalies, Drake Passage, Antarctica.

*Corresponding author: jwkim@sejong.ac.kr

1. INTRODUCTION

Interpreting marine gravity field anomalies is often ambiguous when no sufficient density information is provided. In addition to the horizontal density variations, bathymetrical relief is particularly important for anomaly interpretation where the geology and tectonics of the study area are complicated.

In this study, the utility of the Gravity-Geologic Method (GGM) was investigated to estimate improved bathymetry (i.e., seafloor topography) in the Drake Passage, Antarctica. In the study area, there are irregular, and sparse shipborne measurements of sea floor depth, but uniform and dense satellite altimeter measurements are also available. The GGM was originally developed for predicting depth-to-the-basement of a sedimentary basin overlain by lower density formations with known free-air gravity anomalies (FAGA) and some borehole measurements (Adams and Hinze, 1995; Nagarajan, 1994; Ibrahim and Hinze, 1972).

Fig. 1 shows generalized tectonic features of the Drake Passage, Antarctica, and the shaded box delineates the study area (56.1~57.7° W and 60.25 ~61.25° S). The Drake Passage was formed by the separation of present South America and the Antarctic Peninsula in the Oligocene (Barker and Burrel, 1997). In the study area, there is a structural triple junction composed of the Shackleton Fracture Zone, the South Scotia Ridge, and the South Shetland Trench. All these tectonic features are reflected on the ocean bottom topography and

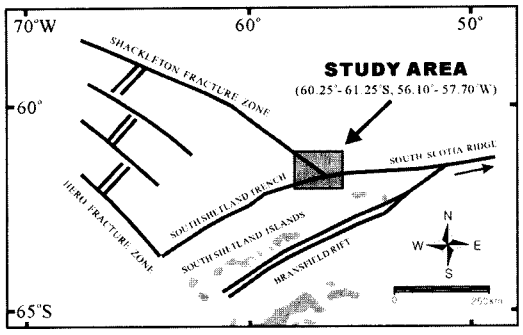

Fig. 1. Generalized tectonic features of the Drake Passage, Antarctica (modified from Jeffers and Anderson, 1990). Shaded box delineates the study area (56.1~57.7°W and 60.25~61.25°S).

local gravity anomalies. Accordingly, interpretation of the gravity anomalies of the study area requires accurate bathymetry and density information (Kim, 1999).

Variations in the local bedrock topography beneath the sedimentary formations generate a relatively short wavelength gravity field compared to the regional gravity field, whereas the more distant mass variations contribute to a longer wavelength gravity field. These two components comprise the observed gravity effects. In the same manner, the regional gravity effects of the ocean floor is estimated by the GGM from known depths, such as are provided by shipborne echo soundings (borehole data for terrestrial applications), and removed from uniform free-air gravity anomalies. These anomalies may be estimated from satellite radar altimetry or measured directly by airborne or shipborne surveys.

For the Drake Passage, the GGM bathymetry was estimated using altimetry-implied FAGA (Sandwell and Smith, 1997) and local bathymetry from Korea Ocean Research & Development Institute (KORDI) shipborne sounding measurements. The FAGA were derived from several altimeter missions including Geosat and ERS1. Local bathymetry was acquired by KORDI's echo soundings during the Antarctic Summer Research Program in Jan., 1993. The GGM bathymetric determinations were compared with bathymetric check values (i.e., bathymetry estimated only from the checkpoints) to determine the statistical improvement that may be available from utilizing the enhanced gravity predictions.

The GGM bathymetry was also compared with other global bathymetry data including the GEODAS (NGDC, 1998), ETOPO5 (NGDC, 1988), and Smith and Sandwell (1997)s model. GEODAS (GEOphysical DAta System) is an interactive database management system developed by the National Geophysical Data Center (NGDC) for use in the assimilation, storage and retrieval of geophysical data. GEODAS contains bathymetric data collected during marine cruises from 1953 to 1998. This worldwide data sources include both U.S. and foreign oceanographic institutions and government agencies (NGDC, 1998). The ETOPO5 was generated from a digital database of land and seafloor elevations on a 5'-by-5' grid. The resolution

of the gridded data varies from true 5'-by-5' for the ocean floors. Smith and Sandwell (1997) released global seafloor topography based on various satellite radar altimeter measurements.

2. GRAVITY-GEOLOGIC METHOD

The Gravity-Geologic Method (GGM) was originally developed for predicting the depth-to-the-basement overlain by lower density sedimentary formation. The depth from the surface to the basement and the observed Bouguer gravity anomalies (BGA), known at control points j_s, are used to produce a regional gravity field (Fig. 2). The regional anomaly field is then subtracted from BGA at all other sites i to generate residuals that may be used to estimate the bedrock undulations.

Variations in the local bedrock topography will generate a related shorter wavelength gravity field g_{RES}, while all other more distant mass variations within the Earth will contribute to a regional gravity field g_{REG}. These two components comprise the observed BGA g_{OBS} given by:

$$g_{OBS}(i) = g_{RES}(i) + g_{REG}(i) \quad (1)$$

The residual bedrock gravity effect g_{RES} is estimated using the following simple Bouguer slab formula:

$$g_{RES}(j) = 2\pi G\Delta\rho\,(E(j) - D) \quad (2)$$

where G is a universal gravitational constant ($6.672 * 10^{-8}\ cm^3/(gm * sec^2)$), $\Delta\rho$ is a density contrast (gm/cm^3), $E(j)$ is a bedrock elevation (m) at j^{th} control point, and D is a reference datum elevation (m).

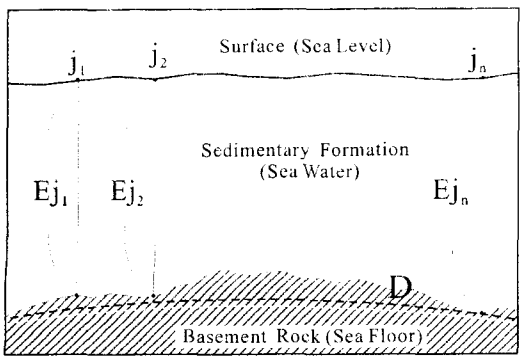

Fig. 2. Geometry of Gravity-Geologic Method.

The bedrock elevations are determined usually by direct measurements (i.e., borehole) through the overlying formations. The deepest measurement is commonly used as the reference datum surface (D). The gravity effect of the bedrock surface at the borehole locations is estimated by Equation 2 and removed from the original BGA values to yield the following regional gravity effects:

$$g_{REG}(j) = g_{OBS}(j) - g_{RES}(j) \quad (3)$$

The depths determined at the borehole sites are interpolated or gridded to generate regional anomalies and removed from the original BGA to generate residual anomalies over the original grid:

$$g_{RES}(i) = g_{OBS}(i) - g_{REG}(i) \quad (4)$$

From the Equations 2 and 4, these residual anomalies can be used to estimate the bedrock surface variations according to:

$$E(i) = g_{RES}(i)/(2\pi G\Delta\rho + D) \quad (5)$$

In general, the accuracy of GGM estimates of bedrock topography are primarily influenced by the number and distribution of elevation control points and the density contrasts between bedrock and the overlying sediments. However, as described by Roman (1998), methods may be readily devised to test these parameters in any application by studying their effects on a subset of the control points.

One of the useful applications for the GGM is predicting the ocean bottom topography. In the marine application, bathymetry predictions are made instead of depth-to-the-basement and FAGA are used instead of BGA, but the process otherwise remains the same. Over ocean areas, FAGA replace BGA because the FAGA are located approximately at the geoid and, hence, do not need to be corrected for free-air and Bouguer slab effects. Also, the assumption of homogeneity in the density contrast across the bedrock interface is more valid in marine than in terrestrial applications. In terrestrial applications, GGM predictions may be seriously distorted because density variations within the overlying formations and bedrock may be the same order of magnitude or greater than the density contrast at the bedrock interface (Ibrahim and Hinze, 1972; Adams and Hinze, 1995; Anderson, 1991; Nagarajan, 1994).

Relative to marine applications, the density contrast between seawater and bathymetry is much more dominant and homogeneous. The utility of the GGM for predicting bathymetry is evaluated in the following section.

3. BATHTMETRY PREDICTIONS IN THE DRAKE PASSAGE

In order to test the veracity of GGM in a deep, rugged ocean bottom environment, the area 56.1~57.7° W and 60.25~61.25° S in the Drake Passage, Antarctica, was selected (Fig. 1). The selected area is well covered with the 2-minute altimetry-implied FAGA by Sandwell and Smith (1997) that were used as observed anomalies g_{OBS} (marked with black dots) and bathymetric data (black lines) from KORDIs shipborne echo soundings (Fig. 3). The shipborne echo sounding measurements were digitized and vectorized from the charts of KORDI. Attributes listed for the map include the Amplitude Range AR of (minimum, maximum), the Amplitude Mean AM, the Amplitude Standard Deviation ASD, the Amplitude Unit AU, and Grid Interval GI. These data provide both the control values necessary to produce the bathymetric predictions along with test values to check the validity of the estimates. Of the 6548 bathymetric measurements for this region, two thirds of these points (4365) were used as control depths, while the remaining values (2183) were used as checkpoints. These

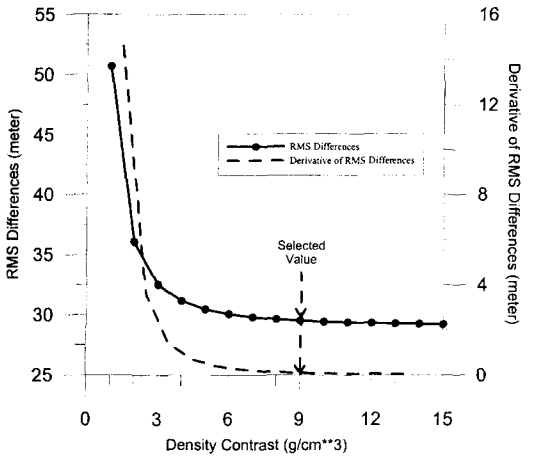

Fig. 4. Trade-off diagram for selecting a density contrast in the study area. Although not a geologically reasonable value, a density contrast of 9.0 gm/cm^3 was selected because the RMS differences between the GGM predictions and the checkpoints converge to 29.2 m as the density contrast is increased.

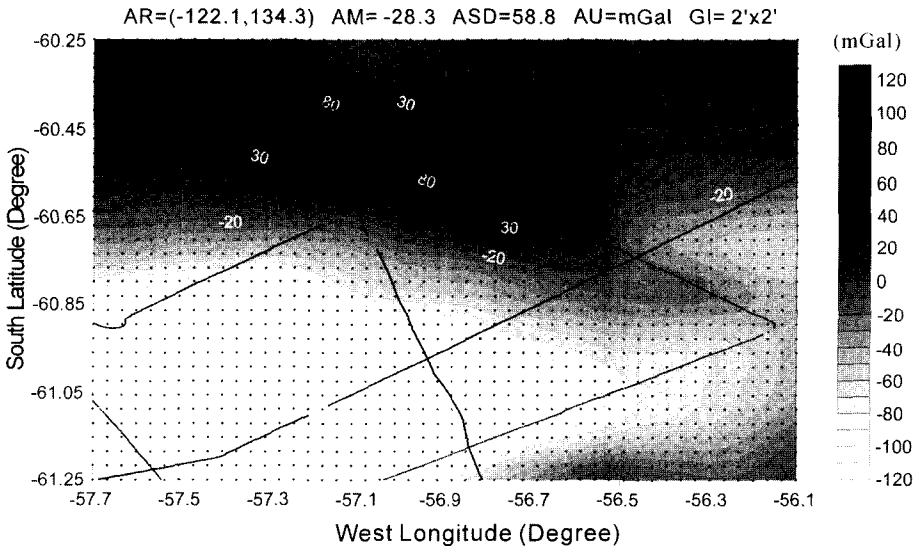

Fig. 3. The 2-minute altimetry-implied free-air gravity anomalies by Sandwell and Smith (1997) and shiptracks for echo soundings by KORDI. The altimeter grid and shiptracks are marked with black dots and black lines, respectively. Of the 6548 points, two thirds of these points were used as control points with the remaining values as checkpoints. Attributes listed for the map include the Amplitude Range AR of (minimum, maximum), the Amplitude Mean AM, the Amplitude Standard Deviation ASD, the Amplitude Unit AU, and Grid Interval GI.

data were collected along profiles where every third point was used as a checkpoint to ensure fairly even distribution of checkpoints across the study area. For the reference datum elevation D in Equations 2 and 5, -5325.94 m (below sea level) was selected.

From Equation 5, an error in the density contrast amplifies errors in the residual gravity anomalies, and, hence, in the resultant bathymetric predictions. Nagarajan (1994) found that the checkpoints could be used to choose an optimum value for $\Delta\rho$ in this kind of application, although it is not geologically reasonable. Fig. 4 is a trade-off diagram for selecting an adequate density contrast for GGM. The trade-off diagram gives variations in RMS difference between the GGM and the check-

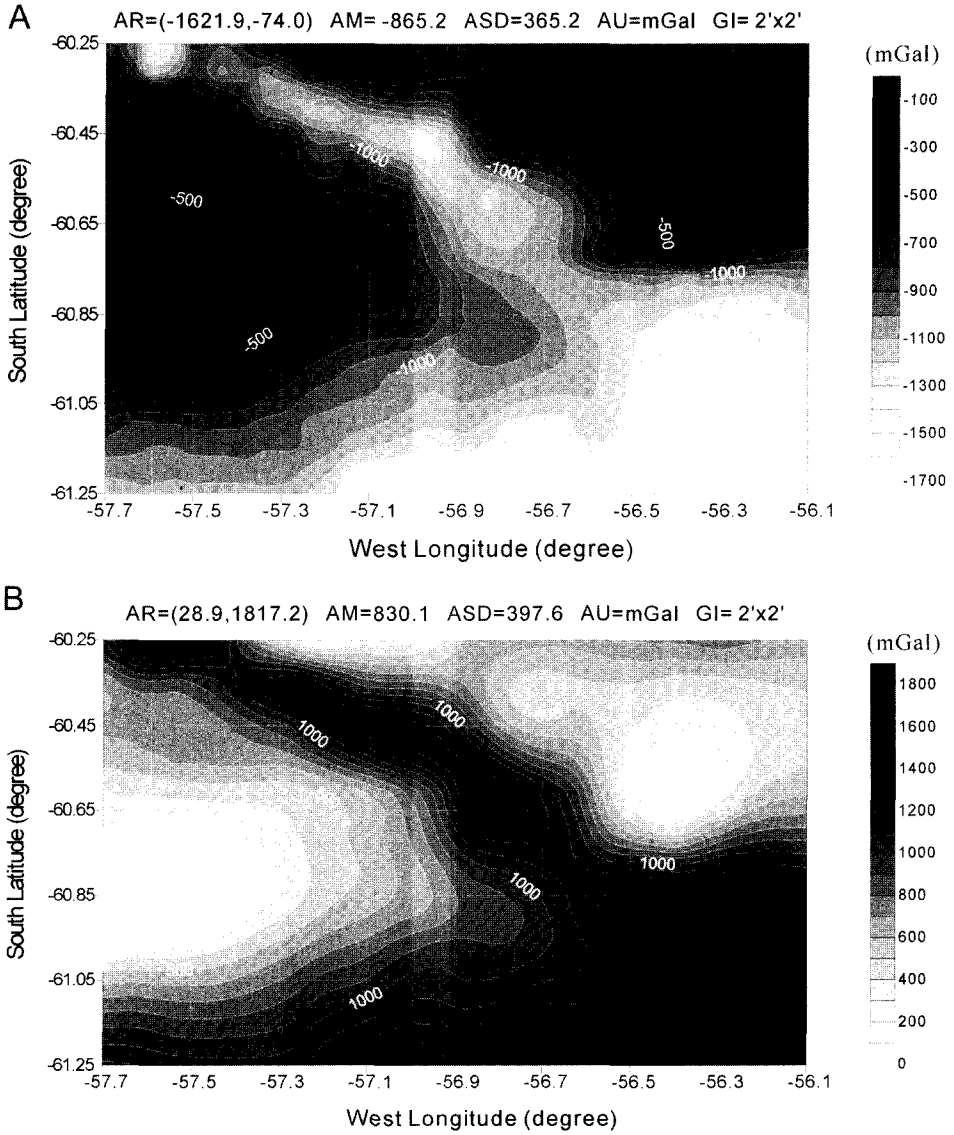

Fig. 5. (A) Regional and (B) residual free-air gravity anomalies. The residual anomalies were estimated by removing the regional gravity anomalies field determined from the control data with a density contrast of 9.0 gm/cm^3 from the free-air gravity anomalies in Fig. 3.

points predictions with changes in the density contrast assumed between the seawater (1.03 gm/cm^3) and ocean bottom topographic mass. Jin (1995) estimated the density of the study area as 2.3-2.7 gm/cm^3, and we selected a maximum value of 2.70 gm/cm^3 for the density of the topographic mass. With the reasonable density contrast of 1.67 gm/cm^3, however, the RMS difference (black solid line with dots) between the two predictions is about 40.0 m. The RMS differences, however, converge to 29.2 m as the density contrast is increased. Therefore, 9.0 gm/cm^3 was selected for the density contrast, $\Delta\rho$, in Equation 5 with the RMS difference of about 29.5 m. In the derivative of the RMS difference shown in the gray broken line, the values converge to zero at the selected contrast. Although not a geologically reasonable value, assuming a density contrast of 9.0 gm/cm^3 permits a higher resolution for determining the ocean bottom topography of the rugged area. Using the selected density contrast of 9.0 gm/cm^3, the regional FAGA were determined from the control points data as shown in Fig. 5A. These regional FAGA were then removed from the FAGA in Fig. 3 to generate a residual FAGA shown in Fig. 5B. These residual FAGA were directly used for the bathymetry prediction given in Fig. 6A. Accordingly, the two gravity anomalies in Fig. 5 show a strong inverse correlation coefficient of -0.96.

The GGM bathymetry in Fig. 6A was estimated from altimetry-derived FAGA with a regular grid spacing of 2 minutes and shipborne soundings with poor coverage in the study area. As a result, the bathymetry was locally well adjusted by the FAGA where no shipborne measurements were found. In the area where shiptracks exist, however, the original sounding values were somewhat distorted and reflected by the application of GGM. Under the assumption that the original shipborne sounding values were more accurate than GGM bathymetry where measurements were made, we merged the original shipborne sounding measurements with the GGM bathymetry in Fig. 6A. All the original shipborne sounding measurements were then directly added to and replaced the GGM bathymetry resulting in an enhanced GGM prediction.

In order to merge the KORDI's shipborne sounding values with the GGM bathymetry, a selective merging technique was developed. The selective merging was implemented to combine high-frequency sparse data (shipborne measurements) and relatively lower-frequency dense data (GGM bathymetry). First, we divided the 2-minute cells of FAGA by 4 in both columns and rows to be 0.5'-by-0.5' cells in order to enhance the resolution. We then switched a FAGA value of the cell with the shipborne sounding value if any shipborne measurements were found within the cell. For the FAGA of the cells around the shiptracks, we either switched or averaged the sounding values after examining the statistics of the components. We decided to use the original FAGA for the remaining cells. Once this procedure was applied to each cell, we regridded bathymetry with the reconstructed cells using a minimum curvature algorithm (Smith and Wessel, 1990) to produce enhanced GGM bathymetry that is the final result of the study. This merging technique, however, can be applied only if the correlation coefficient (CC) and the energy level of the two data sets are very close. In this study, we normalized the GGM data to the shipborne data before they were merged so that the mean (μ) and standard deviation (σ) of the two data are the same (von Frese *et al.*, 1997).

The GGM and KORDI bathymetric predictions in Fig. 6A and B are well correlated (CC=0.91), but they have different energy levels that can be estimated by the σ. This may cause problems in applying selective merging technique. In fact, the σs of the two maps are -1098.4 m (a) and -889.8 m (b), respectively. For detailed comparison, in Fig. 7, we estimated the CCs and σs along the lines of -60.8° S (*Profile #1*) and -56.9° W (*Profile #2*), shown in gray lines in Fig. 6A and B.

Fig. 7 shows the results of comparison with statistics along the yellow lines in Fig. 6A and B, and white lines in Fig. 8A. The black lines with triangle symbols denote bathymetry from sonar soundings, and the gray lines with square symbols denote bathymetry estimated by the GGM in this study. For *Profile #1* in Fig. 7A that is parallel to the latitudinal lines, the two predictions are correlated with a CC of 0.836, but they show significant difference in the averages. For *Profile #2*, the two predictions are better correlated with similar statistics. We normalized the maps in Fig. 6A

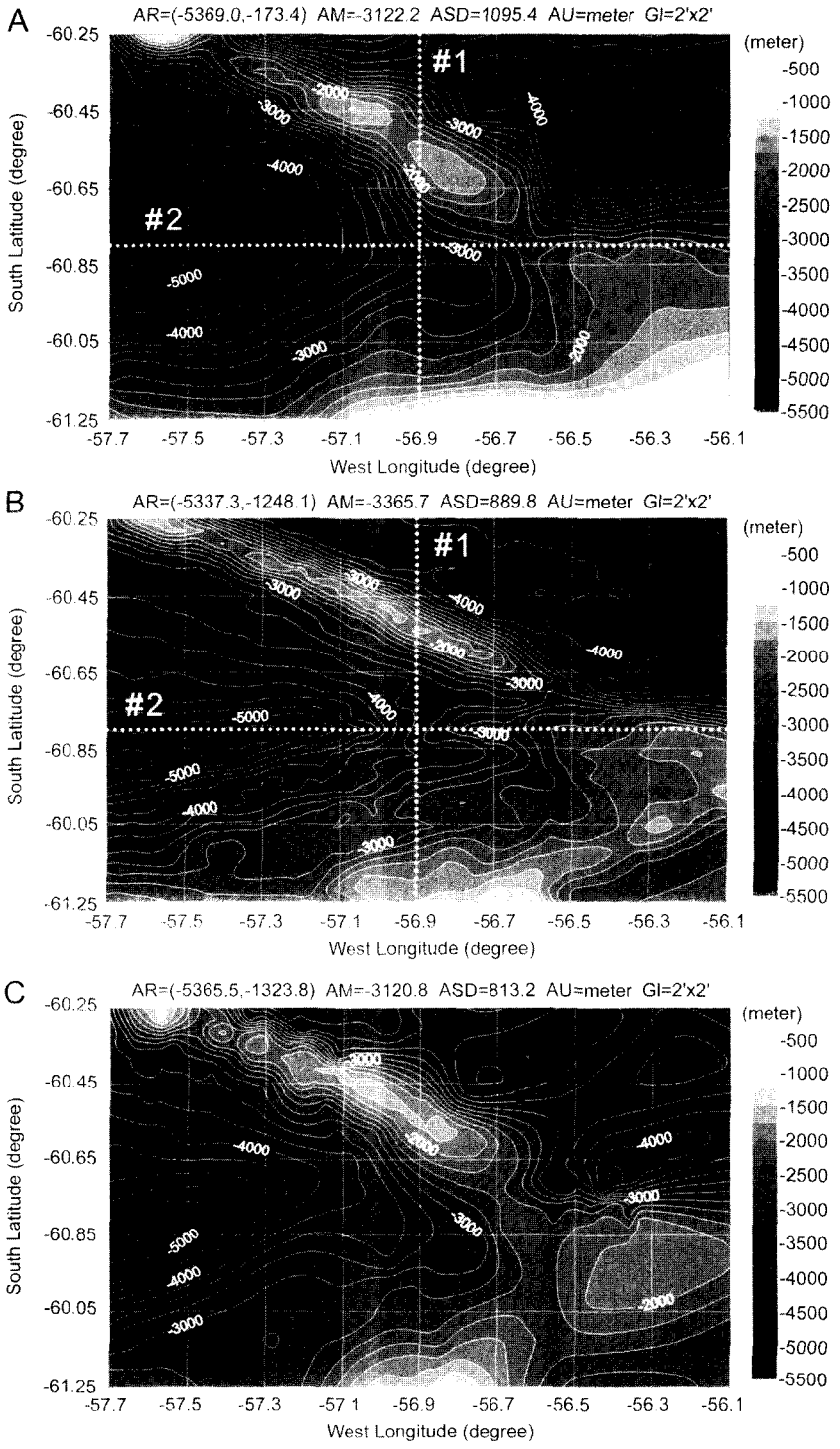

Fig. 6. Bathymetry predictions by (A) Gravity-Geologic Method (GGM), (B) KORDIs echo soundings, and (C) checkpoints values.

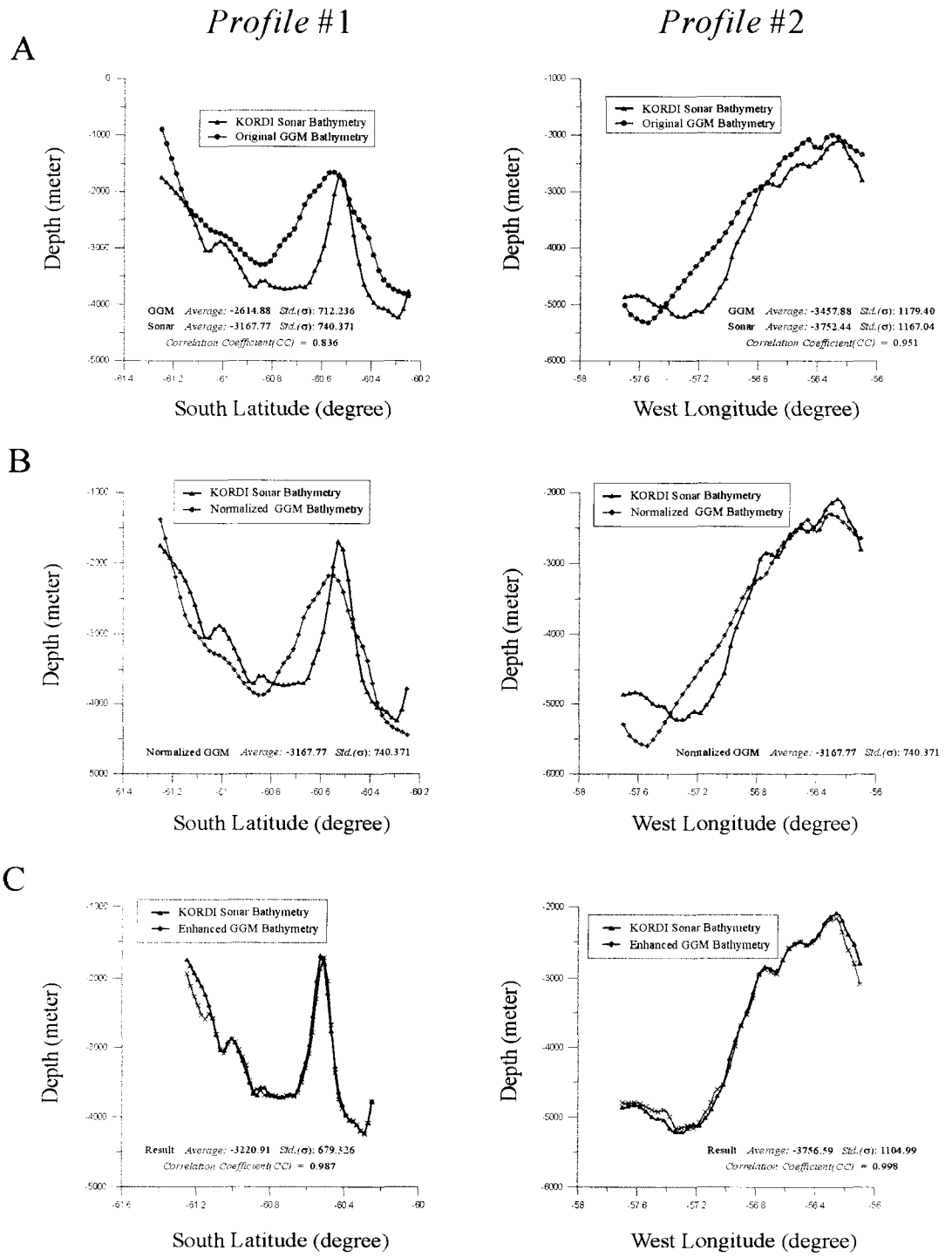

Fig. 7. Comparisons of the GGM-derived and KORDIs bathymetry along the west longitude of 56.9 ° (*Profile #1*) and south latitude of 68.8° (*Profile #2*) that are shown in yellow in Fig. 6. A. KORDIs sonar sounding and original GGM bathymetries, B. KORDIs sonar sounding and normalized GGM bathymetries, and C. KORDIs sonar sounding and enhanced GGM bathymetries by selective merging.

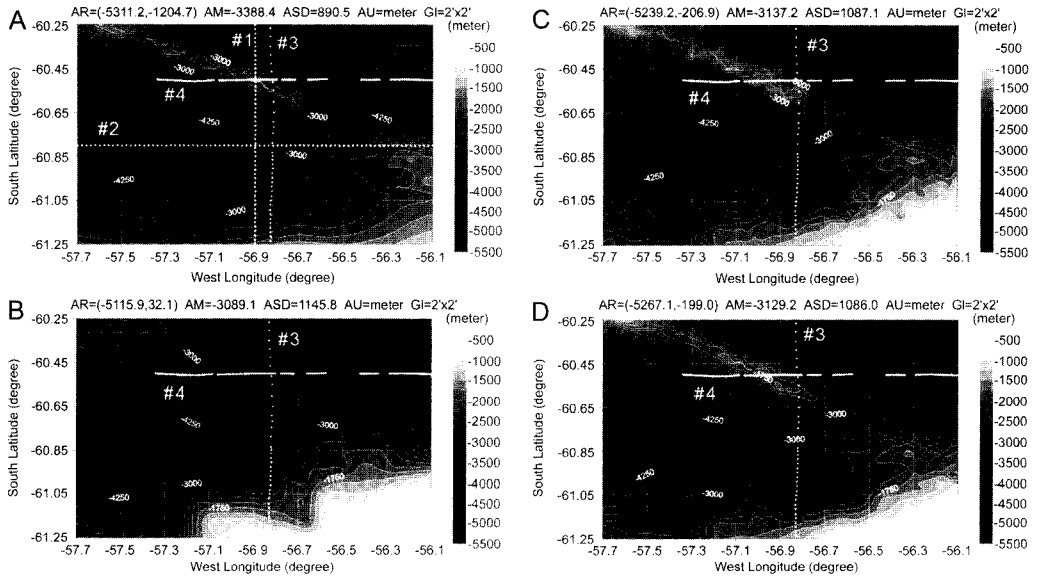

Fig. 8. Comparisons of bathymetry estimated from A. this study (enhanced GGM), B. GEODAS, C. ETOPO5, and D. Smith & Sandwell(1977)'s models.

Table 1. Comparison of correlation coefficients (CC) between the original GGM bathymetry (before selective merging of GGM) and KORDI, Checkpoint, GEODAS, ETOPO5 bathymetries. RMS differences between the GGM, KORDI, and Checkpoint bathymetries are also shown in parenthesis (unit in meter).

BATHYMETRY	GGM	KORDI	Checkpoint	GEODAS	ETOPO5
GGM	1.0	0.91(562.2)	0.89(527.4)	0.92	0.85
KORDI	0.91(562.2)	1.0	0.92(432.7)	0.89	0.80
Checkpoint	0.89(527.4)	0.92(432.7)	1.0	-	-
GEODAS	0.92	0.89	-	1.0	0.91
ETOPO5	0.85	0.80	-	0.91	1.0

and B so that they have an identical μ and σ in order to apply the selective merging technique. In Fig. 7B, the normalized bathymetries are compared along the two profiles. By normalization, the profiles have the same μ of 3167.8 m and σ of 740.4 m. These values were selected based on the original sonar *Profile #1* in Fig. 7A. Note that the CCs were not changed after the normalizations. Finally, using the selective merging technique, we estimated the enhanced GGM bathymetry of the study area shown in Fig. 8A, which is the final result of this study. In Fig. 7C, the two *Profiles #1* and *#2* (shown in white) from enhanced GGM in Fig. 8A shows almost perfect CCs (i.e., 0.99 and 1.0).

As mentioned earlier in this study, two thirds of the KORDIs shipborne measurement points were used as control depths, while the remaining points were used as checkpoints. In Fig. 6C, the bathymetry estimated only from checkpoint values are shown. The RMS difference and CC between GGM and checkpoint bathymetries is 527.4 meter and 0.89, respectively (Table 1). The RMS difference between GGM and KORDI bathymetries (bathymetry estimated by KORDI's shipborne soundings only) is 562.2 meter, which is 6.6% greater than the RMS between GGM and checkpoint bathymetries, indicating the GGM prediction in this study is reliable.

4. BATHYMETRY COMPARISONS

The original and enhanced GGM bathymetries were compared with KORDI bathymetry as well as other global bathymetry data including the GEODAS (NGDC, 1998), ETOPO5 (NGDC, 1988),

and Smith & Sandwell (1997)'s model. First, the original GGM was statistically compared with the KORDI, GEODAS, and ETOPO5 bathymetries in Table 1. The GGM bathymetry shows the CCs of 0.91, 0.92, and 0.85 with KORDI, GEODAS, and ETOPO5 predictions. In deed, the global ETOPT5 has the minimum CC with the GGM, while GEODAS shows the maximum. Overall, the bathem-

Table 2. Comparison of correlation coefficients (CC) between the enhanced GGM bathymetry (after selective merging of GGM) and KORDI, GEODAS, ETOPO5, Smith & Sandwell (1997)'s bathymetries. RMS differences between the bathymetries are also shown in parenthesis (unit in meter).

BATHYMETRY	Enhanced GGM	KORDI	GEODAS	ETOPO5	Smith & Sandwell
Enhanced GGM	1.0(0.0)	0.97	0.948(449.8)	0.852(671.3)	0.954(441.3)
KORDI	0.97	1.0	-	-	-
GEODAS	0.948(449.8)	-	1.0(0.0)	0.911(475.4)	0.986(184.3)
ETOPO5	0.852(671.3)	-	00.911(475.4)	1.0(0.0)	0.909(480.8)
Smith & Sandwell	0.954(441.3)	-	0.986((184.3)	0.909(480.8)	1.0(0.0)

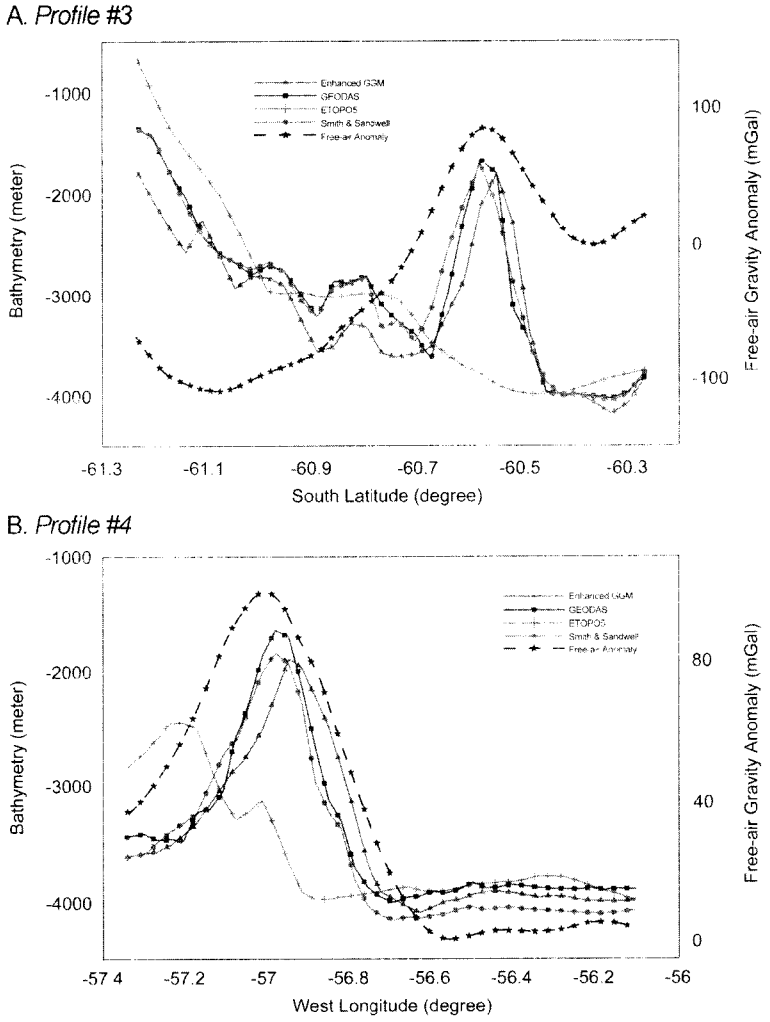

Fig. 9. Profiles of bathymetric predictions and free-air gravity anomalies along the GEODAS shiptracks for A. longitudinal *Profile #3* and B. latitudinal *Profile #4* that are shown in yellow in maps of Fig. 8.

etry predictions show reasonable coherences with each other.

The enhanced GGM was also statistically compared with the GEODAS, ETOPO5, and Smith & Sandwell (1997)s bathymetries in Table 2. The enhanced GGM bathymetry shows CCs of 0.97, 0.948, and 0.852 with KORDI, GEODAS, and ETOPO5 predictions. While CCs with KORDI and GEODAS were increased by 6.6% and 3.3%, respectively, the CC with ETOPO5 remained the same. In Fig. 8, the enhanced GGM (A), GEODAS (B), ETOPO5 (C), and Smith & Sandwell(1977)'s (D) bathymetries are compared. For graphical comparison, they have same color scales and contour intervals. Except the ETOPO5, all three maps show Shackleton Fracture Zone as bathymetric highs of -1500 and -1800 meters, whereas the South Scotia Ridge is appeared in all four maps. The enhanced GGM also shows a CC of 0.954 with Smith & Sandwell's models. The enhanced GGM shows RMS differences of 449.8, 671.3, and 441.3 meters, respectively, with the other GEODAS, ETOPO5 and Smith & Sandwells predictions. The GEODAS and Smith & Sandwells maps are almost identical since most of the GEODAS data could be involved in the Smith & Sandwell's model. The main sources of errors may be density and regularity of the shipborne measurements. KORDI and GEODAS have irregular track coverage and this may cause errors where, in particular, there are not enough sounding values. Moreover, both bathymetric undulations and horizontal density variations contribute to the altimetry-implied gravity anomalies used in this study, and, hence, the resulting altimetry-derived bathymetries are distorted in the study area.

More comparison was made along the GEODAS' ship tracklines that are shown in yellow in Fig. 8. Along the *Profile #3* (parallel to longitudinal line) and *Profile #4* (parallel to latitudinal line), bathymetries as well as FAGA by Sandwell and Smith (1997) are compared in Fig. 9A and 9B. Note that the FAGA along the profiles are shown in different scales and units. Overall, the FAGA show good correlation with bathymetries except at the southern half of the *Profile #3*. The South Shetland Trench and the South Scotia Ridge are located in this region and this geologic and tectonic complex may explain the mismatch between FAGA and bathymetries. In the two profiles, the ETOPO5 model does not reflect the bathymetric high due to the Shackleton Fracture Zone, while all other bathymetries and FAGA show the peak clearly. Again, the Smith & Sandwells and GEODAS models are well correlated in the profiles. The enhanced GGM also shows some peaks and troughs in the two models, and some shifts in amplitudes and phases.

5. CONCLUSIONS AND DISCUSSIONS

The Gravity-Geologic Method (GGM) was implemented for bathymetric determinations in the Drake Passage, Antarctica, using global marine Free-air Gravity Anomalies (FAGA) data sets by Sandwell and Smith (1997) and KORDI's local echo sounding measurements. Of the 6548 bathymetric sounding measurements, two thirds were used as control depths, while the remaining values were used as checkpoints. A density contrast of 9.0 gm/cm^3 was selected based on the checkpoints predictions with changes in the density contrast assumed between the seawater and ocean bottom topographic mass. This value, although geologically unreasonable, was found to generate the best bathymetric predictions

Control depths from the echo soundings were used to determine regional gravity components that were removed from FAGA to estimate the gravity effects of the bathymetry. These gravity effects were converted to bathymetry by inversion. In particular, a selective merging technique was developed to effectively combine the echo sounding depths with the GGM bathymetry to enhance high frequency components along the shipborne sounding tracklines. For the rugged bathymetry of the research area, the GGM bathymetry shows correlation coefficients (CC) of 0.91, 0.92, and 0.85 with local shipborne sounding by KORDI, GEODAS, and a global ETOPO5 model, respectively. The enhanced GGM by selective merging shows improved CCs of 0.948 and 0.954 with GEODAS and Smith & Sandwell(1997)'s predictions with RMS differences of 449.8 and 441.3 meters.

In the study area, FAGA and bathymetries were found not consistent in the complex topographic

area due to geologic and tectonic features such as the South Shetland Trench and the South Scotia. This may be explained by the fact that both bathymetric undulations and horizontal density variations contribute to the altimetry-implied gravity anomalies, and, hence, the resulting altimetry-derived bathymetries are distorted.

In general, the GGM appears to be a sufficient tool for making bathymetric predictions in marine environments. The global marine FAGA data sets and other bathymetric models ensure that the GGM can be used in conjunction with shipborne bathymetry from echo sounding to extend the coverage into the unmapped regions, which should generate better results than simply gridding the sparse data or relying upon lower resolution global data sets such as ETOPO5.

ACKNOWLEDGMENTS

The authors thank Prof. Ralph von Frese at The Ohio State University and Dr. Daniel Roman at NGS/NOAA for their reviews and comments on this paper. Elements of this study were produced with support from 1999-2001 National R&D Program of Korea Ministry of Science & Technology (Energy/Resources 99-03) and from Polar Research Division of Korean Ocean Research and Development Institute.

REFERENCES

Adams, J.M. and W.J. Hinze (1995) The gravity-geologic technique for mapping varied bedrock topography. In Ward S.H. (ed.) Geotechnical and Environmental Geophysics. Society of Exploration Geophysicists, Tulsa, OK, III, p. 99-106.

Anderson, G. (1991) Use of the gravity-geologic method: Error propagation and case study. Unpublished M.S. thesis, Dept. of Geological Sciences, the Ohio State University,.

Barker and Burrel (1997) The opening of Drake Passage. Marine Geology, v. 25, p. 15-34.

Ibrahim, A. and Hinze, W.J. (1972) Mapping buried bedrock topography with gravity. Ground Water, v. 10(3), p. 18-23.

Jeffers, J.D. and Anderson, J.B. (1990) Sequence stratigraphy of the Bransfield Basin, Antarctica, implication for tectonic history and hydrocarbon potential. In St. John, B.(ed.) Antarctic as an exploration frontier hydrocarbon potential, geology, and hazards. Am. Assoc. of Petroleum Geologists Studies in Geology, v. 13, p. 13-29.

Jin, Y.K. (1995) Crustal structure of the South Shetland trench and the Shackleton fracture zone off the northern Antarctic Peninsula. Ph.D. Dissertation, Seoul National University, 140p.

Kim, J.W. (1999) A study on the gravity anomalies in the Drake Passage, Antarctica, using satellite radar altimetry. Report 1999-1, Research Institute of Geoinformatics & Geophysics, Sejong University, 79p.

Nagarajan, R. (1994) Gravity-geologic investigation of buried bedrock topography in northwestern Ohio. MS Thesis, Department of Geological Sciences, The Ohio State University, Columbus, OH.

NGDC (1988) Data Announcement 88-MGG-02, Digital relief of the Surface of the Earth. NOAA, National Geophysical Data Center, Boulder, Colorado.

NGDC (1998) Marine trackline geophysics data CD-ROM set. U.S. Dept. of Commerce, NOAA, National Geophysical Data Center, Boulder, Colorado.

Roman, D.R. (1998) An integrated geophysical investigation of Greenlands tectonic history. Ph.D. Dissertation, Department of Geological Sciences, The Ohio State University, Columbus, OH, 270p.

Sandwell, D.T. and Smith, W.H.F. (1997) Marine gravity anomalies from Geosat and ERS-1 satellite altimetry. J. Geophys. Res., v. 102, B5, p. 10,039-10,054.

Smith, W.H.F. and Sandwell, D.T. (1994) Bathymetric prediction from dense satellite altimetry and sparse shipboard bathymetry. J. Geophys. Res., v. 99, B11, p. 21,803-21,824.

Smith, W.H.F. and Sandwell, D.T. (1997) Global sea floor topography from satellite altimetry and ship depth soundings. Science, v. 277, p. 1957-1962.

Smith, W.H.F. and Wessel, P. (1990) Gridding with continuous curvature splines in tension. Geophysics, v. 55, p. 293-305.

von Frese, R.R.B., Jones, M.B., Kim, J.W. and Kim, J.-H. (1997) Analysis of anomaly correlations. Geophysics, v. 62(1), p. 342-351.

Youn, S.W. (2000) A study on the gravity field of the Drake Passage, Antarctica, using Geosat radar altimetry. MS Thesis, Department of Earth and Environmental Sciences, Korea University, 102p.

2002년 1월 11일 원고접수, 2002년 6월 14일 게재승인.